

Predicting the penetration depth and towing resistance of beam trawl fishing gears in sand

Ghorai, Bithin; Tiano, Justin; Molenaar, Pieke; Soetaert, Karline; Keetels, Geert

DOI

[10.1080/1064119X.2024.2361009](https://doi.org/10.1080/1064119X.2024.2361009)

Publication date

2024

Document Version

Final published version

Published in

Marine Georesources and Geotechnology

Citation (APA)

Ghorai, B., Tiano, J., Molenaar, P., Soetaert, K., & Keetels, G. (2024). Predicting the penetration depth and towing resistance of beam trawl fishing gears in sand. *Marine Georesources and Geotechnology*. <https://doi.org/10.1080/1064119X.2024.2361009>

Important note

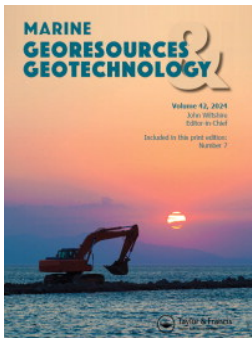
To cite this publication, please use the final published version (if applicable). Please check the document version above.

Copyright

Other than for strictly personal use, it is not permitted to download, forward or distribute the text or part of it, without the consent of the author(s) and/or copyright holder(s), unless the work is under an open content license such as Creative Commons.

Takedown policy

Please contact us and provide details if you believe this document breaches copyrights. We will remove access to the work immediately and investigate your claim.



Predicting the penetration depth and towing resistance of beam trawl fishing gears in sand

Bithin Ghorai, Justin Tiano, Pieke Molenaar, Karline Soetaert & Geert Keetels

To cite this article: Bithin Ghorai, Justin Tiano, Pieke Molenaar, Karline Soetaert & Geert Keetels (24 Jun 2024): Predicting the penetration depth and towing resistance of beam trawl fishing gears in sand, Marine Georesources & Geotechnology, DOI: 10.1080/1064119X.2024.2361009

To link to this article: <https://doi.org/10.1080/1064119X.2024.2361009>



© 2024 The Author(s). Published by Informa UK Limited, trading as Taylor & Francis Group



Published online: 24 Jun 2024.



Submit your article to this journal [↗](#)



Article views: 102



View related articles [↗](#)



View Crossmark data [↗](#)

Predicting the penetration depth and towing resistance of beam trawl fishing gears in sand

Bithin Ghorai^{a,b} , Justin Tiano^{c,d}, Pieke Molenaar^c, Karline Soetaert^d and Geert Keetels^a

^aOffshore and Dredging Engineering, Maritime and Transport Technology Department, Faculty of Mechanical Engineering, Delft University of Technology, Delft, The Netherlands; ^bPresent affiliation: Department of Ocean Engineering, Indian Institute of Technology Madras, Chennai, India; ^cWageningen Marine Research, Wageningen University & Research, Wageningen, The Netherlands; ^dDepartment of Estuarine and Delta Systems, Royal Netherlands Institute for Sea Research, Den Burg, The Netherlands

ABSTRACT

Accurate characterization of mechanical perturbations on the seabed is essential for developing models assessing the environmental impacts from physical disturbances. Furthermore, understanding the relationship between (1) seabed resistance and (2) penetration depth, can also facilitate the development of more efficient and less impactful fishing gears. This study examines these two aspects of tickler chain rigged beam trawling *via* large-scale physical experiments. Three scaled down models (“light,” “medium,” and “heavy” designs) were developed to represent the impacts from typical beam trawl configurations used in the North Sea and were towed at various speeds on a saturated sand bed. Results reveal that increasing the towing speed reduces the mean penetration depth and the steady-state towing resistance of the gears. Smaller scale physical model tests incorporating tickler chains in sand, demonstrate that the towing resistance is significantly influenced by the soil compaction and particle sizes. Moreover, our study offers a simple and efficient method to estimate the penetration depth and towing resistance of prototype beam trawl gears in sand. This approach, along with the associated research, may be valuable for marine scientists assessing trawling impacts and demersal fishing gear designers seeking to optimize efficiency while minimizing seabed disturbance.

ARTICLE HISTORY

Received 25 November 2023
Accepted 11 May 2024

KEYWORDS

Beam trawling; tickler chain; seabed disturbance; penetration depth; towing resistance; experiment



1. Introduction


The demersal fishing sector in the North Sea has experienced many challenges in the previous decades such as the construction of wind farms and associated subsea infrastructure built on fishing grounds, and strongly fluctuating fuel prices. Additionally, the largest fishing fleet in the North Sea, the Dutch demersal fishery, has been adversely affected by the European ban on electric pulse fishing, which forced the fishery to return to less efficient catch methods such as traditional beam trawl fishing rigged with “tickler chains” (Kraan et al. 2020). Consequences of this development are believed to result in larger benthic disturbance and fuel consumption (van Marlen et al. 2014; Rijnsdorp et al. 2020). A more complete understanding of the seabed resistance associated to beam trawl gears would aid in identifying optimization procedures used to reduce the penetration depth and resistance.

Beam trawling targeting demersal fish species generally involves a vessel sailing at approximately 4.5–7 knots speed (Eigaard et al. 2016), with a towed funnel-shaped net deployed on the seabed. The net is held open by a steel

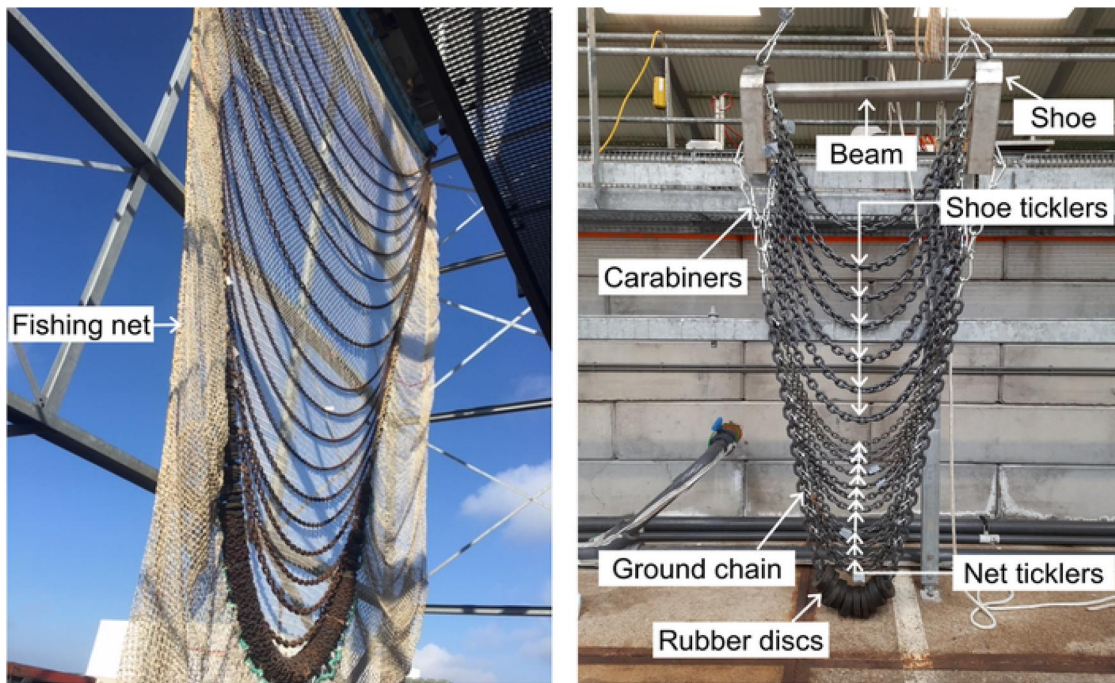
framework, containing a tubular beam (4.5–12 m in length) and a pair of trawl heads at each end termed as “shoe.” A set of chains connected to the shoes known as “shoe tickler,” and a set of chains tied to the ground rope called “net tickler,” are used to stimulate the fish to come out of the sediment and be caught by the net. The ground rope consists of a heavy chain and rubber discs (with varying diameter and thickness) encircling the chain near the centre (Figure 1). The purpose of the ground rope is threefold: (1) to maintain bottom contact and prevent escaping of the fish below the net, (2) to keep the net damage free and safe during trawling and (3) to ensure fish is pushed by the water flow over the ground rope and captured in the net. During towing, the seabed is disturbed due to the physical interaction between the trawl components (trawl shoes + shoe tickler chains + net tickler chains + ground rope + net) and the sediment.

Marine species living on or inside the seabed can be strongly impacted by trawling activity. The penetration depth of demersal fishing gears can be used to predict the depletion of macrofauna in the seabed (Hiddink et al. 2017), as well as trawl-induced biogeochemical impacts (De Borger

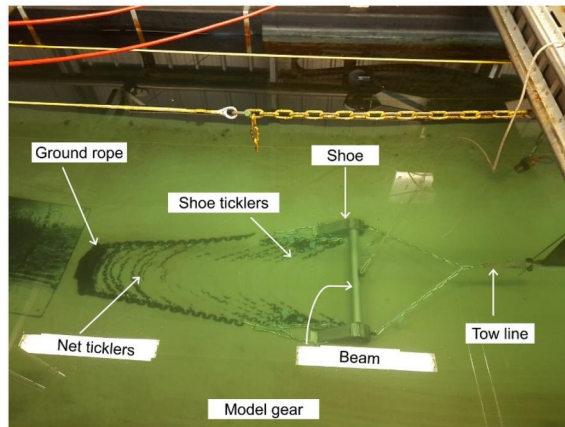
CONTACT Bithin Ghorai  bghorai@iitm.ac.in  Department of Ocean Engineering, Indian Institute of Technology Madras (IITM), Chennai, India.

 Supplemental data for this article can be accessed online at <https://doi.org/10.1080/1064119X.2024.2361009>.

© 2024 The Author(s). Published by Informa UK Limited, trading as Taylor & Francis Group
This is an Open Access article distributed under the terms of the Creative Commons Attribution License (<http://creativecommons.org/licenses/by/4.0/>), which permits unrestricted use, distribution, and reproduction in any medium, provided the original work is properly cited. The terms on which this article has been published allow the posting of the Accepted Manuscript in a repository by the author(s) or with their consent.



(a)



(b)

Figure 1. Beam trawl configurations: (a) full-scale heavy configuration in air (left side) and model heavy configuration gear setup (width 1 m) outside the water basin (right side), and (b) model gear inside the water tank facility prior to towing.

et al. 2021). Several studies have tried to measure the penetration depth of trawl gear by using site-scanning and placing markers in the trawl track by SCUBA divers (Anonymous 1990; Bergman and Hup 1992; Bridger 1972; De Groot 1995; Lindeboom and De Groot 1998; Margetts and Bridger 1971; Paschen, Richter, and Köpnick 2000). Depestele et al. (2016) considered both field experiments and numerical modelling. The mean penetration depth observed in the field for beam trawl gear components ranges from 0.3 to 8 cm, depending on the seabed sediment type (fine to medium to hard sandy soil) of the fished area (see Table S5 for details) and gear components (Eigaard et al. 2016). Although studies have estimated the footprint and resuspension caused by bottom fishing gears across broad spatial scales in accordance to subsurface penetration (Eigaard et al. 2016; Rijnsdorp et al. 2021), further investigation into diverse chain configurations and sailing speeds

would enhance on the mechanisms behind the variation in penetration depths exhibited within fishing gear types.

An important issue with beam trawl fishing is energy usage. In addition to the inherent resistance of the fishing vessel moving through the water, the drag caused by towing (“tow resistance”) can impose a heavy energy demand on the vessel. Tow resistance is a combination of the hydrodynamic forces on the beam and net, and the friction forces induced by the interaction of the beam shoes, ground rope and tickler chains with the seabed. The hydrodynamic resistance of the fishing net and gear elements have been well documented (Bi et al. 2014; Depestele et al. 2019; O’Neill and Ivanović 2016; Prat et al. 2008; Rijnsdorp et al. 2021; Tang et al. 2017, 2018), however, only limited information can be found on the geotechnical interaction of the fishing gear with the seabed (Esmaili and Ivanović 2014, 2015; Ivanović and O’Neill 2015; Ivanović, Neilson, and O’Neill

2011). The majority of these seabed-focused studies examined the physical interaction between a single disc or rock-hopper and the soil. Though Enerhaug (2011) conducted small-scale model tests with a single chain element, interactions among multiple tickler chains (typical of beam trawling) with the soil have not yet been considered. It is, therefore, crucial to examine and quantify the physical impact of tickler chain rigged beam trawl gears towed across the seabed to properly assess their impacts on seafloor integrity and marine ecosystems.

In this study, we determined the penetration depth and tow resistance induced by tickler chains on sand using three typical beam trawl configurations. The data was obtained from a series of large-scale experiments with scaled models (1 m width) in an indoor towing tank on a sandy bed. From these data, we developed empirical relations for the prototype gears for the estimation of penetration depth and tow force as a function of chain diameter and tow velocity. These relations are helpful as input for ecological models (De Borger et al. 2021; Hiddink et al. 2017) and the prediction of vessel engine power (Rijnsdorp et al. 2000). The effects of seabed density and soil particle size on the towing resistance were also investigated by performing additional experiments with smaller scale models (~ 20 cm width).

2. Materials and methods

2.1. Large-scale experimental procedure

Large-scale physical experiments were conducted in the towing tank facility available at the Visserij-innovatiecentrum Zuidwest-Nederland B.V. (VIC) in Stellendam fishing port, Netherlands, to investigate the gear penetration and associated drag resistance during beam trawling. A schematic of the experimental setup with scaled beam trawl gear in the test basin is illustrated in Figure 2. The prototype dimensions of beam trawl gear elements were first collected from the fishery experts [Visserij Coöperatie Urk (VCU) and Coöperatie Westvoorn (CW) Stellendam] and then analysed to build model trawl gears. An example of the prototype light gear elements is summarized in Table 1 (for shoe tickler chains and net ticklers) and Table 2 (for ground rope components), and the corresponding details of the model gear are listed in Table 3 (see Tables S3 and S4 for medium and heavy chain gear configurations, respectively). Three different scale model configurations (light, medium and heavy chain pattern) were built in the workshop of the Royal Netherlands Institute for Sea Research (NIOZ). The physical model trawl configurations represented scaled down versions of the range of gear weights (see details in Table 4) encountered in practice in the Netherlands. All the gear components – beam (with shoes), tickler chains (shoe and net ticklers) and ground rope (with rubber discs) were scaled down by a length factor $\lambda_L = 12$. This factor and the overall size of the models were chosen to minimize boundary effects in the water tank (3.2 m width, 33 m length, 2 m height), and lowered the risk of potentially exceeding the maximum towing capacity of carriage.

Another factor to consider is the diameter of each chain link as they all collectively exert a nearly constant pressure onto the seabed. Albiker et al. (2017) suggested that the scale effects for offshore monopile foundations in sand due to soil particle size could be neglected if the pile diameter is relatively large compared to the mean grain diameter. We used a similar strategy in our experiments to scale down the size of the chain links for beam trawl models. The chain link diameter (d) was proposed to be significantly greater than the mean particle size of sand grains (d_{50}) for minimal scale effects. The measured mean particle size of Quartz sand in the VIC towing tank was $d_{50} = 0.4$ mm. For this study, we scaled down the chain link diameter d by a factor $\lambda_D = 2$, resulting in d/d_{50} ratio in the range of ~ 15 – 40 (Figure S1). This ratio is relatively high, ensuring minimal scale effects. The two different scale factors (λ_L and λ_D) for tickler chains were chosen (Enerhaug et al. 2012) to suitably utilize the maximum towing capacity of the carriage while mimicking the trawl gear response close to reality. An example of the model heavy gear setup prior to testing in the water tank is shown in Figure 1.

2.2. Penetration depth measurement

To measure the average penetration of gears onto the sand bed, a simple yet effective method was devised using aluminium foil markers. Sets of five markers (10 cm length \times 2 cm width) were fastened, ~ 10 cm apart, onto a 50 cm metallic bar which was placed into the trawling path perpendicular to the towing direction (Figure 2). Prior to each test run, SCUBA divers carefully pushed the bar and foil marker arrangement into the sand with the markers positioned vertically inside the sediment allowing the upper edge of the foil marker to be aligned with the sediment-water interface. After each test run, the markers were recovered from the sand bed *via* SCUBA. The trawling disturbance caused wrinkles and deformities to appear onto the upper sections of the foil markers whereas the lower undisturbed sections remained smooth and glossy (Figure S2). The distance of the “disturbance length,” on each individual foil marker, was estimated to the nearest mm. This involved measuring from the area closest to the sediment water interface (the top of the foil marker) to the point at which evidence of disturbance (scratches and wrinkles) ceased to be visible on the foil marker (Figure S2). This disturbance “penetration” depth is assumed to encompass both the depth of sediment displacement (and resuspension) and the depth of mixing beneath the displaced sediment (De Borger et al. 2021; Depestele et al. 2019).

The horizontal marker “position” (markers 1–5 from left to right on the metal bar; Figure S3) was included as a random effect variable in generalized linear mixed models (GLMM). These models assessed whether penetration depth was significantly affected by weight and speed, with penetration depth as the dependent variable and “mass” (in kg) and “velocity” (in knots) of the gear specified as fixed effects (Bolker et al. 2009). The *glmer*-function in the R package “lme4” (Bates et al. 2015) was used to create each GLMM,

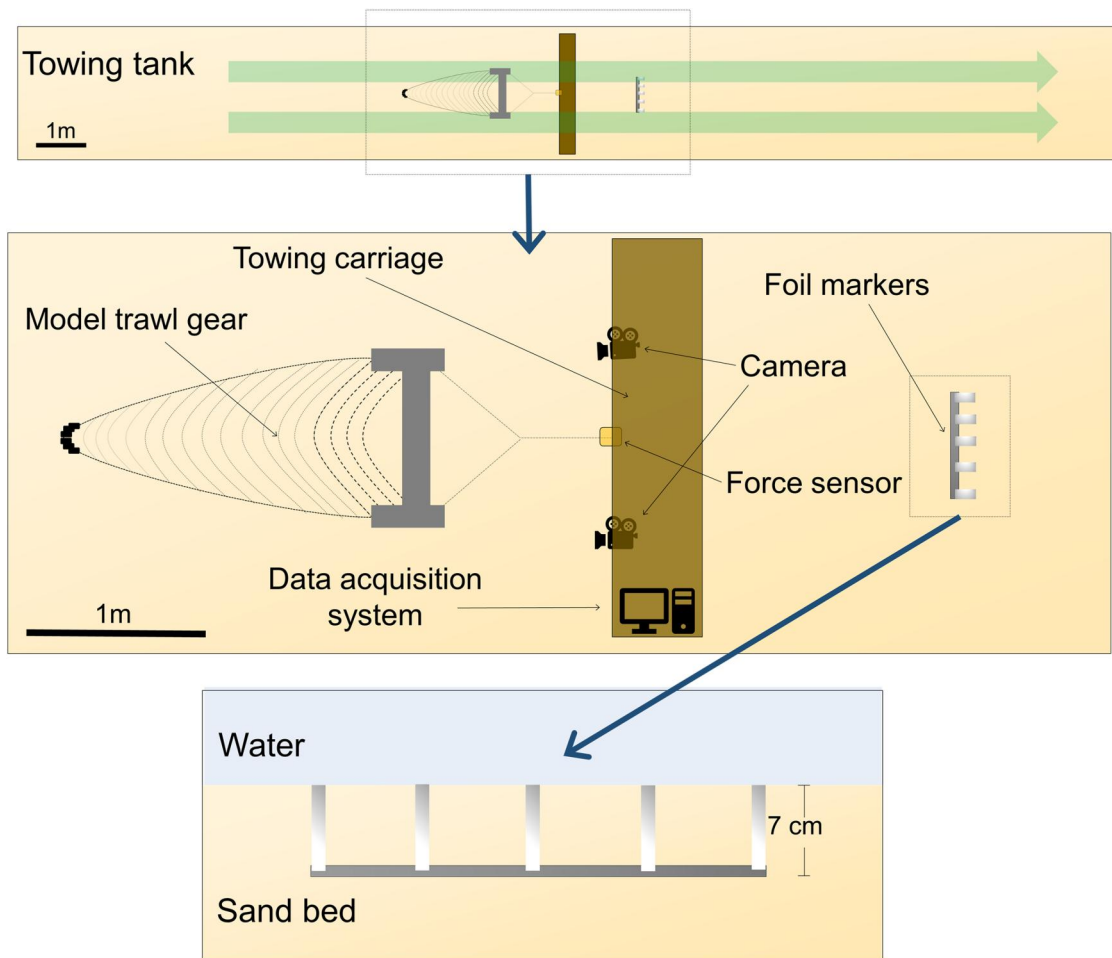


Figure 2. Schematic of the towing tank facility with the model beam trawl gear system and experimental-set up (top view) used at the Visserij-innovatiecentrum Zuidwest-Nederland B.V. (VIC) in Stellendam, Netherlands. The bottom panel shows a side view of how experimental foil markers were placed into the sand bed.

Table 1. An example of a light weight full scale gear configuration in the North Sea (VC Urk, The Netherlands).

	Chain length (m)	Chain link diameter (mm)	Unit mass of chain (kg/m)	Chain link type ^a (short/long)	Chain link inner length (mm)	Chain link inner height (mm)
Shoe ticklers						
1	16	16	5.9	Short	45	16+7
2	17.5	16	5.9	Short	45	16+7
3	19	16	5.9	Short	45	16+7
4	20.5	16	5.9	Short	45	16+7
5	22	16	5.9	Short	45	16+7
6	23.5	16	5.9	Short	45	16+7
7	25	16	5.9	Short	45	16+7
Net ticklers						
1	15	11	2.75	Short	31	11+7
2	14	11	2.75	Short	31	11+7
3	13	11	2.75	Short	31	11+7
4	12	11	2.75	Short	31	11+7
5	11	11	2.75	Short	31	11+7
6	10	11	2.75	Short	31	11+7
7	9	11	2.75	Short	31	11+7
8	8	11	2.75	Short	31	11+7
9	7	11	2.75	Short	31	11+7
10	6	11	2.75	Short	31	11+7
11	5.5	13	3.75	Short	36	13+7
12	5	13	3.75	Short	36	13+7
13	4	16	5.9	Short	45	16+7
14	4	16	5.9	Short	45	16+7

^aChain link dimensions are a function of the link diameter, outside link length $\sim 6d$ and outside link height $\sim 3.35d$. Long link chains feature link which exceed a length of $6d$.

Courtesy: UR W22 Rev. 6 CLN, 2016, Offshore mooring chain, International Association of Classification Societies, U.K.

Table 2. An example of a full scale ground rope configuration in the North Sea (CW Stellendam, The Netherlands).

Ground rope components	Length (m)	Diameter of chain link/ rubber disc (mm)	Chain link inner length (mm)	Chain link inner height (mm)	Mass of chain/ rubber disc in air (kg)	Mass of chain/ rubber disc in seawater (kg) = 1/6th of the mass in air
Ground chain	34.6	30mm	108	30 + 7	145	24.2
Rubber disc (in the centre portion of the gear)	3.0	300 (90 mm gap between each disc)	–	–	4029	671.5
Rubber disc (on the sides of the gear adjacent to centre discs)	2.5	200, 240, 260, 280 (from outside to inside)	–	–		

Table 3. Details of light weight model gear used in large-scale experiments (VIC stellendam).

	Chain length (m) ($\lambda_L = 12$)	Chain link diameter (mm) ($\lambda_D = 2$)	Unit mass of chain (kg/m) ($\lambda_m = 4$)	Chain link ^a type (short/long)
Shoe ticklers				
1	1.33	8	1.48	Short
2	1.46	8	1.48	Short
3	1.58	8	1.48	Short
4	1.71	8	1.48	Short
5	1.83	8	1.48	Short
6	1.96	8	1.48	Short
7	2.08	8	1.48	Short
Net ticklers				
1	1.25	6	0.69	Short
2	1.17	6	0.69	Short
3	1.08	6	0.69	Short
4	1.00	6	0.69	Short
5	0.92	6	0.69	Short
6	0.83	6	0.69	Short
7	0.75	6	0.69	Short
8	0.67	6	0.69	Short
9	0.58	6	0.69	Short
10	0.50	6	0.69	Short
11	0.46	7	0.94	Short
12	0.42	7	0.94	Short
13	0.33	8	1.48	Short
14	0.33	8	1.48	Short

^aChain link dimensions are a function of the link diameter, outside link length $\sim 6d$ and outside link height $\sim 3.35d$.

Long link chains feature link which exceed a length of $6d$.

Courtesy: UR W22 Rev. 6 CLN, 2016, Offshore mooring chain, International Association of Classification Societies, U.K.

Table 4. Details of model beam trawl gears used in large-scale experiments.

Model trawl gear configuration (source of the reference gear)	Mass of the whole gear in air (kg)	Mass of (tickler chains + net ticklers + ground rope) in air without the beam and carabiners, M_{dry} (kg)	Mass of (tickler chains + net ticklers + ground rope) in seawater without the beam and carabiners, M_{wet} (kg)	Tow velocity in knots (m/s)
Light chain pattern (VC Urk)	~ 74.4	~ 47.0	~ 40.8	2 (1.0), 3 (1.5), 4 (2.1)
Medium chain pattern (CW Stellendam)	~ 91.8	~ 64.4	~ 55.9	2 (1.0), 3 (1.5), 4 (2.1)
Heavy chain pattern (CW Stellendam)	~ 110.0	~ 82.6	~ 71.7	2 (1.0), 3 (1.5), 4 (2.1)

for which gamma distributions resembling the residual error structure of the data were incorporated. A log-link function was used to account for non-linearity between predictor and response variables.

2.3. Towing force measurement

A data acquisition (DA) system comprising of a force transducer, amplifier and computer setup was connected to the carriage to record and measure the seabed drag resistance at a given tow velocity. The strain-gauge based force sensor

(S-type) was capable of measuring up to ~ 3 kN load and was calibrated with known masses prior to the use in the experiment. The soil drag load during towing was transferred from the gear-soil interface to a towing rope, connected almost horizontally with the beam of the model gear, and then to a vertical rope tied with force transducer through a pulley with the aid of a steel beam arrangement. Towing experiments were carried out using a carriage that supports this system (see Figure 3 for the instrument setup). The expected towing force is approximately 5–10% higher than the recorded force due to the resistance of the pulley

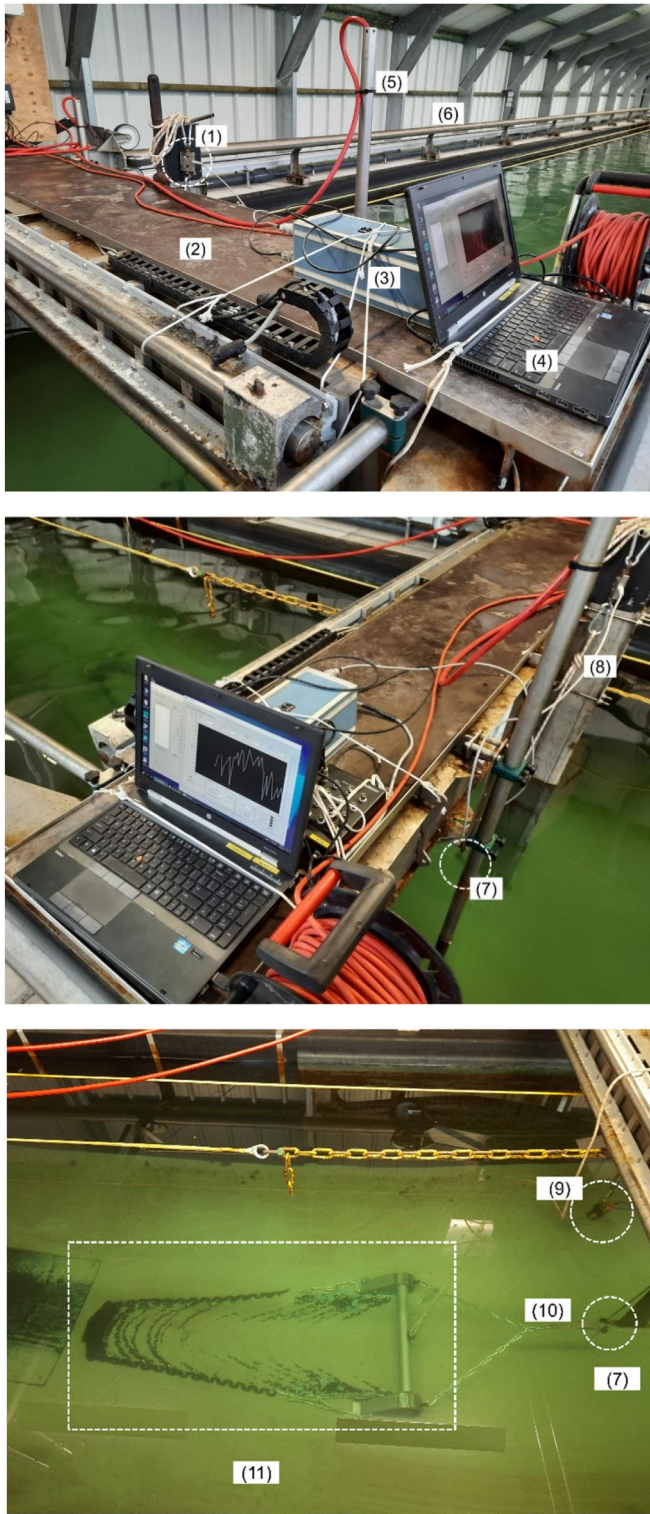


Figure 3. Instrument set-up and test facility – different components: (1) force transducer, (2) mobile carriage, (3) amplifier, (4) laptop, (5) camera holder with power cable, (6) guide rails, (7) pulley, (8) vertical beam, (9) underwater camera, (10) tow line, (11) model trawl gear.

(verified from tension load tests on the pulley). In addition, 10% random variations are expected in relation to the uncertainty of the force transducer, variable tension in the ropes, acceleration of the gear and fluctuations in the hydrodynamic and geotechnical resistance (bed variations) during the tow, which not completely cancel out in the averaging

process due to relatively short towing period and limited number of repetitions. The measured force-time history response was recorded and stored for each test run in the DA system for analysis.

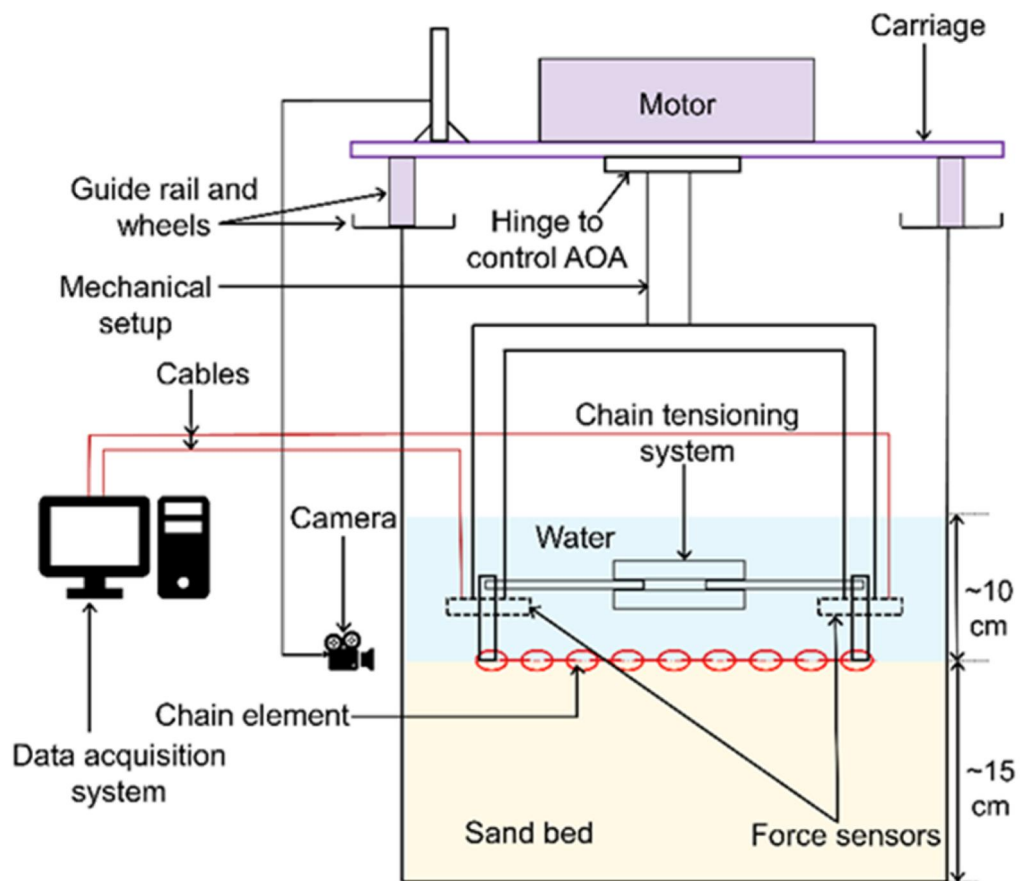
2.4. Small-scale experiments

Small-scale models with sections of tickler chain (length ~ 20 cm) were developed and tested in the water flume facility (filled with sand) available at the Delft University of Technology (TU Delft), Netherlands to study the effects of soil compaction and particle size on the towing resistance as controlling these parameters in the large-scale experiments was not feasible due to the enormous size of the towing basin (33 m long, 3.2 m wide and 2 m deep). The relative density (D_R) is a measure of the degree of compaction of a cohesionless soil which is governed by the in-situ void ratio (e), and the void ratios in the loosest (e_{\min}) and densest (e_{\max}) possible packing. The index D_R is determined experimentally by measuring these void ratios, given by:

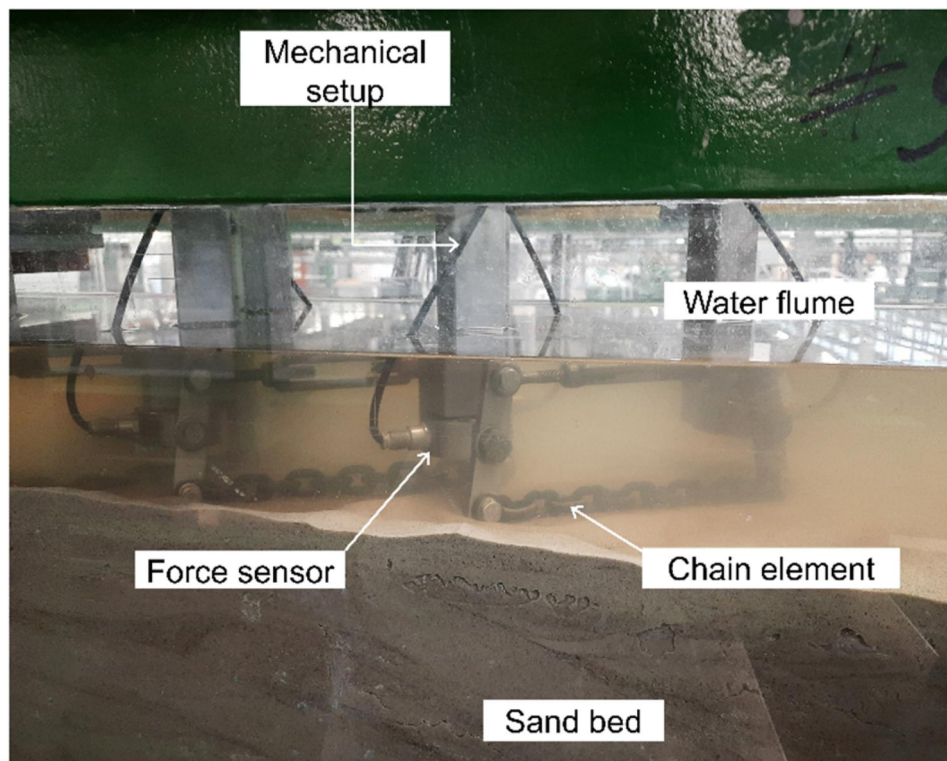
$$D_R = \frac{e_{\max} - e}{e_{\max} - e_{\min}} \times 100\% \quad (1)$$

We varied the void ratio from $e_{\min} = 0.67$ to $e_{\max} = 0.96$, giving dry densities ranging between $\rho_{d,\min} = 1343 \text{ kg/m}^3$ and $\rho_{d,\max} = 1583 \text{ kg/m}^3$. The *in-situ* void ratio was determined as $e = 0.71$, resulting in a relative density index $D_R \sim 85\%$, indicating dense sand behaviour during shearing (Das 2010). To explore the effect of soil relative density, the bed was compacted with a vibration needle. The densification process resulted in a decrease in the height of the sand bed due to reduction in the soil void ratio. The particle size effect was explored by using two different types of industrially processed silica sand in the test basin (supplied by Sibelco from Belgium) – Mol 32 or M32 (coarse-grained) and Mol 34 or M34 (fine-grained) sand. The mean particle sizes (d_{50}) of these coarse- and fine-grained sand samples were 0.26 and 0.17 mm, respectively and the corresponding bulk densities were 1500 kg/m^3 and 1400 kg/m^3 .

A mobile carriage with guide rails was installed on top of the flume to tow the chains. The experimental setup was quite like the one reported in Enerhaug (2011); however, modified for studying multiple chain element interactions with the sand bed. A schematic representation of the test setup along with laboratory arrangements is shown in Figure 4. Three sets of pre-tensioned chains, constrained in the vertical position (i.e., fixed penetration during the tow process), were used in the experiment. The chain link diameters ($d = 6\text{--}16$ mm) were the same as that used in the large-scale experiment, however, the length was adjusted to ~ 20 cm to fit inside the water flume facility (length scale factor $\lambda_L = 60$). As the chain link diameter was sufficiently large compared to the mean grain diameter ($d/d_{50} \sim 23\text{--}62$), scale effects related to soil particle sizes were considered negligible. A constant velocity with three different values ($v = 0.1, 0.3$ and 0.6 m/s) was used. The tow resistance of the chain elements was measured with three pairs of water-resistant force transducer (IP68 rating, maximum load



(a)



(b)

Figure 4. Small-scale experiment set-up at TU Delft: (a) schematic representation, and (b) test arrangement in the water flume facility.

capacity of ~ 1 kN), connected to the ends of the individual chain element. To record force signals from the sensors, a DA system was installed. The whole experiment was shot using a high-resolution video camera, connected to the mobile carriage. Prior to each test run, the bed height (relative density) was maintained constant along the flume length, and the top surface was smoothed out for accurate measurements. After initial preparations, the carriage with the chain system was towed along the sand bed over a sufficient distance (~ 3.4 m) to mobilize steady state drag resistance. The variations in tow resistance with time were measured and examined.

3. Results

3.1. Penetration depth measurements

The average depth of penetration measured (mean \pm standard deviation) was 1.0 ± 0.54 cm, 1.5 ± 0.64 cm and 1.8 ± 0.69 cm for respective light, medium and heavy configurations. Within each gear configuration, slower speeds (2 knots [~ 1.0 m/s]) displayed slightly but consistently higher mean penetration compared to faster speeds (4 knots [~ 2.1 m/s]; Figure 5). When accounting statistically for the differences caused by the marker position (distance from the centre of the trawl track) GLMM's show significant effects for both gear configuration weight ($p < .001$) and towing speed ($p < .001$; Table S1).

3.2. Scaling of penetration depth

The gear penetration depth (z_p) is influenced by several parameters, such as the diameter of tickler chains (d), tow velocity (v), gravitational acceleration (g), density of gear material (ρ_{gear}) and soil bulk density (ρ_{soil}). From a

dimensional perspective this implies that three nondimensional groups can be formed as the problem is controlled by six variables and three fundamental units (mass [kg], length [m], time [s]). We define the following three groups:

- i. The first group represents the measured gear penetration depth normalized with a representative diameter (Equation 2). Figure 5, as confirmed by the GLMM analysis, demonstrates that the penetration depth is controlled by both gear type and tow speed. Given that the chain links of the shoe ticklers apply greater pressure on the soil compared to the net ticklers, it is inferred that these chain links achieve deeper penetration. Hence, we opt to use the diameter of the shoe tickler chains as the representative diameter for this analysis.

$$\Pi_1 = \frac{z_p}{d} \quad (2)$$

- ii. The second group represents the ratio of inertia versus the gravitational forces (Froude number):

$$\Pi_2 = \frac{v}{\sqrt{gd}} \quad (3)$$

- iii. The third group represents the density of the gear material relative to the soil bulk density:

$$\Pi_3 = \frac{\rho_{\text{gear}}}{\rho_{\text{soil}}} \quad (4)$$

As we require an expression for z_p , the experimental data should be used to determine the relation:

$$\Pi_1 = f(\Pi_2, \Pi_3) \quad (5)$$

However, in this study, we investigated the effect of tow speed on different gear configurations (light, medium,

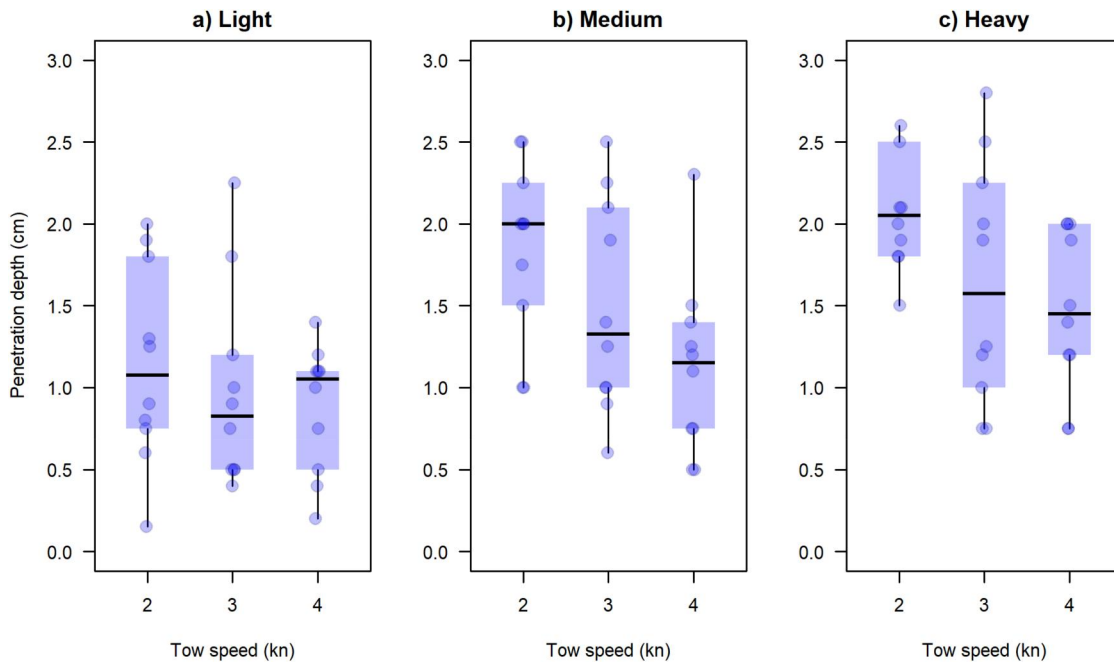


Figure 5. Penetration depth of model gears as a function of tow speed: (a) light configuration, (b) medium configuration and (c) heavy configuration.

heavy) but only for one given soil type (sand) and density (loose). Therefore, the effect of Π_3 could not be considered in the dimensional analysis and it should be borne in mind that the gear penetration is a function of the soil type (sand, mud, gravel, etc.) and compactness of the seabed (medium dense to dense sand). It is, thus, important to study different sediment types and seabed conditions in future research to be able to use this methodology in different environmental conditions. Figure 6 shows the dependence between the two nondimensional groups Π_1 and Π_2 . It can be observed from Figure 6 that all the data seem to fall on a consistent master curve as described by the following scaling relation:

$$\frac{z_p}{d} = c_1 + c_2 \left(\frac{v}{\sqrt{gd}} \right) \quad (6)$$

where, the coefficients $c_1 = 2.04$ and $c_2 = -0.15$ were obtained by linear regression analysis ($R^2 \sim 0.85$).

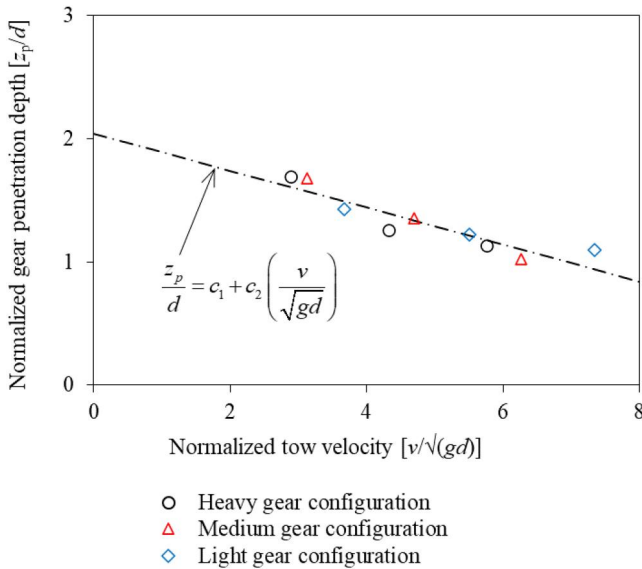


Figure 6. Normalized penetration depth of tickler chains at different normalized tow speeds.

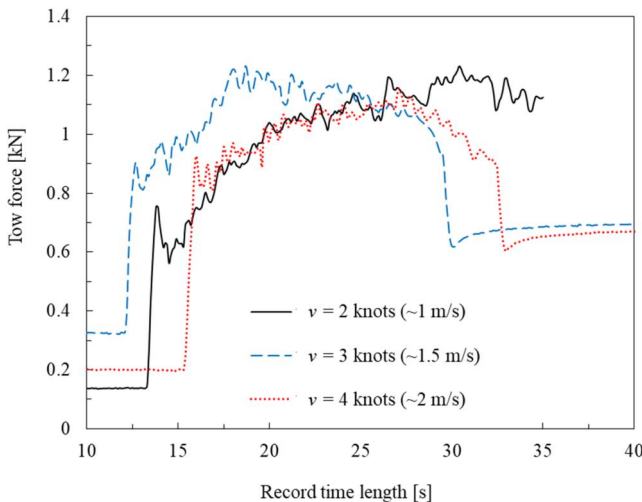
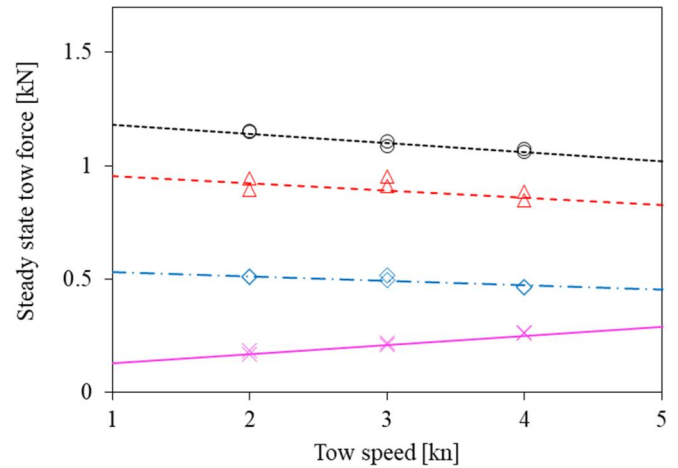


Figure 7. Towing force time trajectory at different speeds for heavy gear configuration.

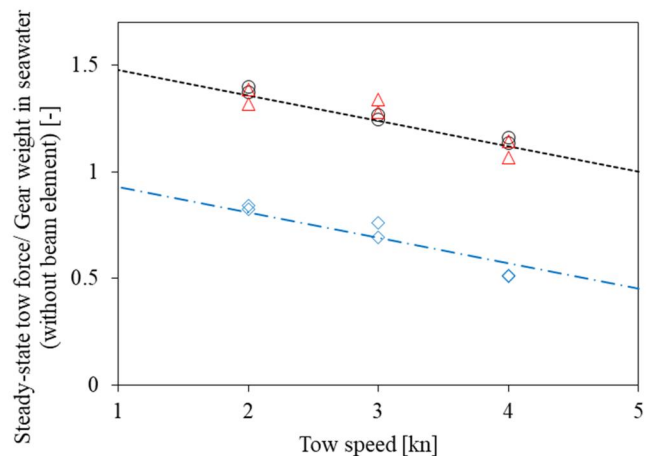
3.3. Measurements of the towing resistance

The seabed resistance during trawling is presented in Figure 7 for a heavy gear configuration towed at speeds $v=2, 3$ and 4 knots (equivalent to $\sim 1.0, 1.5$ and 2.1 m/s). It was observed that the resistance response immediately reaches a peak from the initial value (corresponding to the tension in the towing rope) due to acceleration in the carriage, then stabilizes over a short period of time and finally decreases due to braking. Similar trends were also noticed with other gear configurations and tow speeds. The steady-state tow resistance was estimated from the curves considering the mean value between two arbitrary selected time periods, where the resistance variation is considered negligible across



- Heavy gear configuration
- △ Medium gear configuration
- ◇ Light gear configuration
- × Beam element

(a)



- Experiment - heavy gear
- △ Experiment - medium gear
- ◇ Experiment - light gear
- Linear fit - heavy & medium gear
- .-.- Linear fit - light gear

(b)

Figure 8. Steady-state soil drag resistance at different tow speeds: (a) for entire gear set-up, (b) normalized with respect to the wet weight of tickler chains and ground rope.

the test runs for different gear patterns. The average of the steady resistances is plotted against the tow speed in Figure 8(a) for different model gear configurations. It is interesting to notice that the seabed drag resistance decreases with an increase in speed. This indicates that the gear elements were continuously pushed out of the seabed when dragged at greater speeds – leading to the path of least resistance and associated failure mechanisms in soil. The phenomenon was also verified from penetration depth measurements at different speeds (see Figure 4), where the model gear penetrates less into the soil at greater speeds, involving less volume of soil surrounding the gear component and thus mobilizing low drag resistance. Additional tests were performed considering only the beam element of the model gear to compute the combined drag resistance of shoe tickler chains and ground rope with net ticklers. The contribution from the beam was separated from the total steady-state resistance and then normalized with respect to the submerged weight of the shoe tickler chains, net ticklers and ground rope in seawater (see Figure 8b) for different gear patterns. The normalization of these steady-state resistances for heavy gear configuration resulted in a narrow band of values, and therefore, expressed using a linear curve as shown in Figure 8(b). The normalized soil resistances for other gear configurations with the best-fit lines are also shown in the same figure.

3.4. Scaling of towing force

The scaling of the towing force with respect to the gear submerged weight appears to work reasonably well for the medium and heavy gear configurations but not for the light configuration (Figure 8b). The towing force F is controlled by several parameters: mass of the gear in air (M_{dry}), bulk density of soil (ρ_{soil}), seawater density (ρ_{water}), width of the gear in the tow direction (L), total number of shoe and net tickler chains (n), penetration depth (z_p), tow speed (v) and gravitational acceleration (g). We improved the scaling relationship by considering the individual component that contributes to the total tow force F expressed as:

$$F = K_1 F_w + K_2 F_{pp} + K_3 F_d \quad (7)$$

where the coefficients K_1 , K_2 and K_3 represent the friction factors, respectively due to the submerged weight of the gear in seawater (F_w), passive pressure from the soil mass surrounding the gear (F_{pp}) and the dynamic force due to acceleration of the soil mass in front of the gear (F_d), given by:

$$F_w = M_{dry} g \left(1 - \frac{\rho_{water}}{\rho_{gear}} \right) \quad (8)$$

$$F_{pp} = n \left[(\rho_{soil} - \rho_{water}) L z_p^2 g \right] \quad (9)$$

$$F_d = n \left[(\rho_{soil} - \rho_{water}) v^2 L z_p \right] \quad (10)$$

In the above equations, M_{dry} is the measured mass of the gear components without the beam (see Table 2); ρ_{gear} , ρ_{soil} and ρ_{water} are the densities of gear material, soil and

seawater, respectively, taken as 7800, 1700 and 1030 kg/m³; n is the total number of chains in a particular gear configuration ($n=21$ for the light pattern and $n=18$ for the medium and heavy pattern), $L=1$ m; z_p is the measured mean penetration depth in soil; v denotes the tow speed (m/s) and $g=9.81$ m/s² is the gravitational constant. The contribution from the gear weight (F_w) is significantly higher compared to the passive pressure force (F_{pp}) due to negligible changes in the soil volume surrounding the gear when steady-state resistance was mobilized. The friction factors, that were used to best estimate the total drag force, were determined using a linear regression analysis with multiple variables. The overall regression was found to be good ($R^2 \sim 0.96$, $p < .001$) giving values of $K_1 \sim 0.94$ ($p < .001$), $K_2 \sim 5.2$ ($p < .1$) and $K_3 \sim 0$ ($p < 0.05$). It can be thus inferred that the dynamic force contribution (F_d) was insignificant compared to the other two components while computing the total steady-state drag force (F). The predicted values of the tow force were back calculated using Equation (7) and plotted against the measured values from the experiment in Figure 9. We observed that the predictions are in good agreement with the actual measurements with a standard error limited to $\sim 15\%$.

3.5. Effect of soil parameters on towing resistance

The towing resistance in two different soil grains (M32 and M34 type) for the loose and dense bed condition are compared in Figure 10. For a given velocity, chain diameter and penetration depth, it was observed that the steady-state force required to tow the chains is almost similar for the two different grain sizes in loose bed condition ($D_R \sim 0\%$). However, in dense soil bed, with higher relative density ($D_R \sim 85\%$), the average towing force increased substantially (nearly 2.7 times) when dragged over fine-grained particles compared to coarse-grained particles. Given the expected range of the velocity, penetration depth and soil type we expect drained soil behaviour (Verruijt 2006). For drained conditions, it is known that the effective friction angle (ϕ') strongly depends on the relative density (D_R) of the soil.

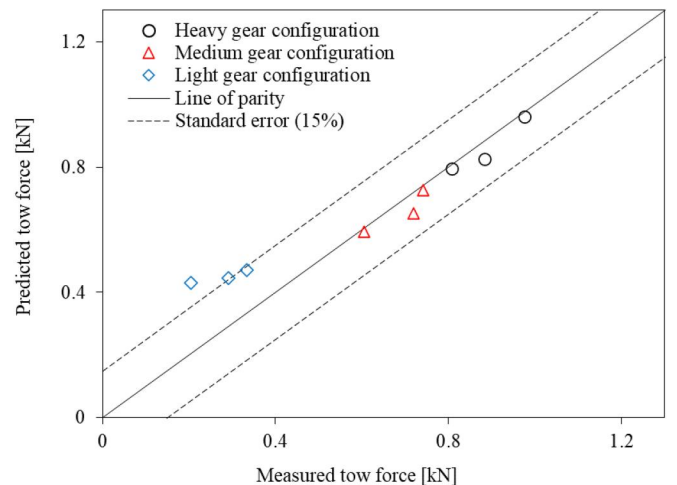


Figure 9. Predicted tow force versus actual tow force measured from experiments.

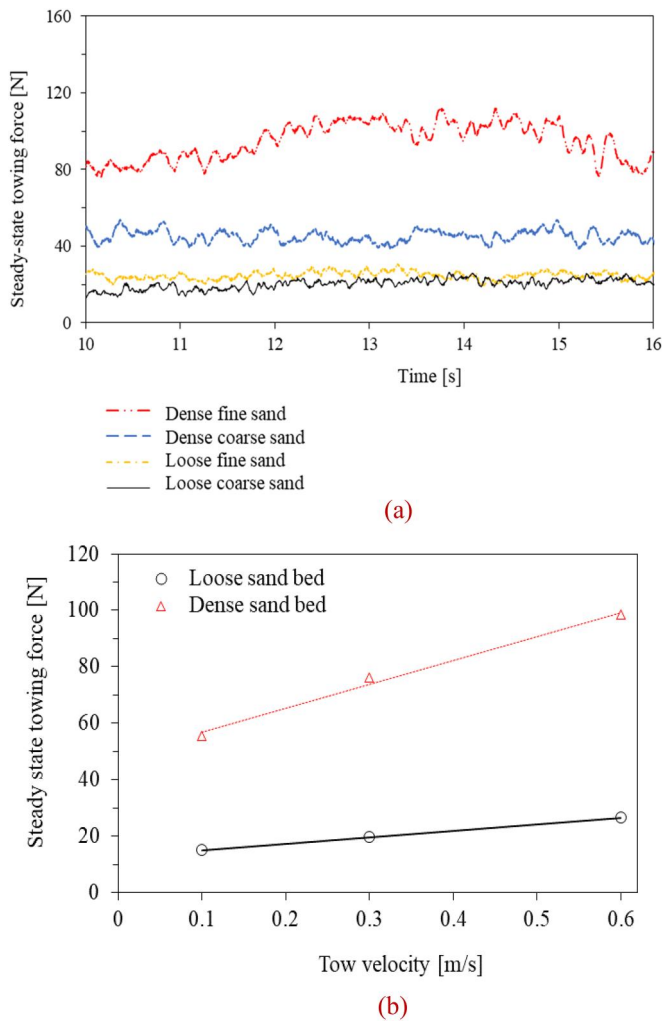


Figure 10. Variation in steady-state towing forces ($d = 6$ mm, $v = 0.3$ m/s): (a) for different soil relative density and mean particle size, and (b) at different velocity.

This effect is of particular importance at low effective stress (Bolton 1986; Chakraborty and Salgado 2010) and is more pronounced in fine-grained sand than coarse-grained sand (Prakash et al. 2023). Since the chains operate in the top layer, the effective stress is in the range of 100–1000 Pa only. An increase of the relative density can result in a substantial increase of the passive soil pressure in front of the chain and thus the towing resistance in sand (Cathie and Wintgens 2001; Depestele et al. 2016).

The average steady-state forces were also evaluated at different tow speeds for a given soil relative density in saturated fine sand and the variations are shown in Figure 10(b). It was observed that the towing resistance in dense fine sand is enhanced by ~ 3.7 times compared to the loose fine sand due to change in the void ratio of the bed by $\sim 44\%$. The soil bed in the large-scale experiments at VIC Stellendam can be considered loose as the sediments were not compacted unlike the small-scale model tests in Delft and it is, therefore, practical to ignore particle size effects on the mobilization of soil drag resistance. In beam trawling, this might often represent the seabed condition as the top layer of the sediment is regularly sheared by waves and

currents, thereby creating a loosely packed fishing ground. Nevertheless, it is notable that the relative density and sediment sizes of the seabed could influence the towing resistance significantly and therefore, it should be considered in the prediction of total drag load on bottom trawl gears.

4. Discussion

4.1. Comparison of penetration depth with field scale measurements

The penetration of prototype beam trawl gear components in sandy sediments was predicted as per the scaling relation proposed in Equation (6). Greater disturbance with heavier gear configurations is expected due to the larger pressure exerted on the soil mass by the gear components (shoe tickler + net tickler chains) causing deeper sediment penetration compared to the lighter chain configurations (Figure 5). The reduced seabed penetration linked with higher speeds is attributed to the lift force acting on the gear components during towing and granular interaction with the seabed. The modelled penetration depth ranges from approximately 1.4 cm to 4.5 cm. The lower penetration value corresponds to a light chain configuration (16 mm shoe ticklers) dragged at 6 knots (~ 3.1 m/s) speed and the higher penetration is for the heavy configuration (26 mm shoe ticklers) towed at 2 knots (~ 1.0 m/s). The modelled penetration depth estimates are compared with available results in the literature based on field scale experiments and sea trials for similar fishing gear components and ground conditions (Table S5). While there is limited information on beam trawl gear components towed on a sandy seafloor at different speeds and chain configurations (weights/number of chains), we found that our predictions are in well agreement with general penetration depth values reported in the literature (1–8 cm; Lindeboom and De Groot 1998; Paschen, Richter, and Köpnick 2000; Valdemarsen et al. 2007). Sea trials with accurate measurements of towing speed on the seabed and collection of good quality samples for soil characterisation remains a challenge to scientists and could possibly corroborate and improve our prediction models in the future.

4.2. Contribution of individual gear components on penetration depth

Variations in observation across different measurement locations along the width of the trawl gear were noted; however, no significant evidence suggests a substantial variance in penetration depth. Nonetheless, it is plausible that differences arise due to variations in the angle of attack of the tickler chains over the width of the gear and the configuration of the ground rope. Throughout our experimental trials, the ground rope remained consistent, enabling us to assess the collective impact of ticklers and ground rope. It is conceivable that the measured results reflect a combined influence of ticklers and the ground rope, rather than solely attributable to ticklers.

Determining the specific chain link or rubber disc responsible for the deepest penetration at each line in the trawl path is not possible from the present data. Rubber discs in the centre part of the gear mitigate pressure by distributing weight of the ground rope over a wider area. Additionally, they may induce a hydrodynamic lifting force, aiding in supporting the ground rope in the central section (Zdravkovich 1985). Therefore, it can be expected that in the central part the shoe ticklers achieve maximum penetration rather than the heavier ground chain. Conversely, at the edges where the tickler chain lacks protection, the ground chain may achieve maximum penetration, owing to the larger pressure induced by the ground chain links. However, caution is warranted with this speculation as the angle of attack of the ground chain is very small in this area, and it remains uncertain whether this will result in less or more penetration. It is plausible that chains with a larger angle of attack remove more soil and consequently achieve greater penetration depth. At the edges, sediment mobilized by shoe ticklers may not have sufficient time to resettle before the arrival of the ground chain, potentially promoting ground chain burial there. This would still imply that the diameter of the tickler chains controls the penetration depth of the gear at the edges of the trawl path. This phenomenon is less likely in the central area due to greater spacing between shoe ticklers, allowing sediment resettlement before the arrival of subsequent chains and finally the ground chain. This would imply that the maximum penetration is achieved by shoe ticklers.

Despite this consideration, since we did not vary the ground chain configuration, we cannot formally exclude that the results are insensitive for the choice of ground chain. Thereby, remarking that the choice of the ground chain in our test is in line with fishery practice and scaled to the laboratory scale with the same scaling factor as applied for the shoe and net ticklers. Our current data allows only speculative insights regarding the mechanistic contribution of ground rope, shoe and net ticklers; a revised study design incorporating tests of individual chains and combinations, alongside more precise penetration depth measurements, is essential for robust conclusions in this direction.

4.3. Translation of tow force measurements to practice

This study allows the prediction of the penetration depth and expected towing force on a prototype scale using a combination of Figure 6 and Equation (7). The towing force ranges from approximately 1824 kg (light gear configuration at six knots speed [~ 3.1 m/s]) to 4445 kg (heavy gear configuration at 2 knots [~ 1.0 m/s] speed). The power consumed by these gear components ranges from approximately 22 kW to 108 kW (the low value corresponds to the light configuration at two knots speed and the high value is for heavy gear towed at six knots speed). It is important to note that the predictions do not account for the resistance of the beam, trawl shoes and the net that can contribute significantly to the power consumption of the beam trawler (Lindeboom and De Groot 1998). Further research focusing

on the resistance and penetration depth of other gear components would enhance our understanding of the comprehensive physical effects of beam trawling with tickler chains.

Rijnsdorp et al. (2021) used the additive impact of multiple gear components to estimate effects of bottom trawling on sediment mobilization in the North Sea. A potential “next step” for experimental gear penetration-based research could be to evaluate the physical effects of different fishing gears and gear components to gain a more holistic perspective of bottom trawl effects. Ultimately, the choice to use light or heavy gears depends on various factors (e.g., sediment type, seabed density, tidal current, fuel consumption, fuel price and catch efficiency) resulting in differing levels of towing forces and seabed penetration. The introduction of higher engine power in the Dutch beam trawl fleet (>221 kW power class sub-fleets) allowed fishers the capacity to tow heavy gears at greater speeds (Rijnsdorp et al. 2008). This created a competitive advantage for fast towing vessels that produced higher catches while preventing potential entrapment in soft sediments (Lindeboom and De Groot 1998; Rijnsdorp et al. 2008). Our study shows that faster towing speeds can reduce seabed penetration, though the use of heavier gears to maintain contact with the seafloor may offset this effect. We acknowledge that fishers sometimes desire the deeper penetration to capture species such as sole which are known to bury themselves in the seabed.

The results from these experiments add nuance to the discussion on the topic of bottom trawl impacts along the seafloor. Gear penetration depth is often generalized by gear type and their components to provide broad estimates of bottom fishing impacts at regional and global scales (Eigaard et al. 2016; Pitcher et al. 2022). We demonstrate how towing speed is an integral factor controlling the seafloor penetration and associated drag resistance of fishing gears. Our results can enhance accuracy to upscaled estimates of gear-specific environmental impacts if towing speed information is available. Adding this type of information to models of sediment mobilization that include towing speed (Rijnsdorp et al. 2021) may lead to a more comprehensive understanding of the physical effects exerted by bottom trawl gears.

5. Conclusion

Our study gave insights regarding the mechanical impact of beam trawl fishing gears with tickler chains on sandy soil. Specifically, large-scale experiments allowed us to create new predictive models of seabed penetration and associated drag resistance as a function of towing speed and gear type. Scaling relations were derived based on a simple dimensional analysis, that could help users in the fishing community to assess the soil disturbance in terms of penetration depth, and trawler engine power in terms of geotechnical capacity of the seabed. The specific conclusions from the study are:

1. The gear penetration into the soil reduces with the increase in tow speed.

2. The penetration depth scales with Froude number and diameter of shoe tickler chains.
3. The steady-state tow force scales with the submerged weight of the gear and weight of the soil mass in front of the chains. There is no direct inertia effect on the steady drag resistance, only *via* the penetration depth as a function of the tow speed.
4. The seabed drag resistance is linked with the gear penetration depth to translate results from model tests to prototype scale.
5. The modelled penetration depth of prototype beam trawl gear elements ranges from ~ 1.4 cm (16 mm tickler chain gear, six knots [~ 3.1 m/s] speed) to ~ 4.5 cm (26 mm tickler chain gear, two knots [~ 1.0 m/s] speed).
6. The towing resistance of prototype gear components (without the fishing net) on sandy sediment was predicted in the range of ~ 1.8 tonnes (light gear, two knots [~ 1.0 m/s] speed) to 4.4 tonnes (heavy gear, six knots [~ 3.1 m/s]), with a maximum error limited to $\sim 15\%$.

The results presented in this article can be used to estimate gear penetration depth and towing resistance in loose sandy seabed. The smaller-scale tests showed that the towing force strongly depends on the soil compaction and particle size distribution, and therefore, it is necessary to consider the seabed with different initial relative densities and grain sizes in future studies. Though sandy soils are the most relevant for the North Sea, it is also useful to study other sediment types such as mud and gravel to support benthic ecological trawl disturbance models (Hiddink et al. 2017) and biogeochemical models looking at the seabed impact (De Borger et al. 2021). In addition, numerical modelling could be helpful to encompass a wide range of parameters, study the effect of different individual gear components and find ways to reduce the seabed impact and fuel waste while maintaining catch efficiency.

Acknowledgements

The work is part of a collaborative research by TU Delft and NIOZ in the Netherlands with support from two NWO projects: Numerical modelling of demersal fishing net systems for design optimization (FishNetSim, project number 18529) and Bottom fishery impact assessment tool (BFiAT, project number 18523). A special thanks to Julia van Beinum for her expert SCUBA skills which were used to obtain penetration depth information. We are very grateful to Robbert whose practical assistance and knowledge of the Dutch fishing sector helped out immensely with the experiments. We give a big thanks to the Visserij-innovatiecentrum Zuidwest-Nederland B.V. (VIC) in Stellendam for allowing us clumsy scientists to perform experiments in their facilities. Our sincere thanks to Niels Koorn for his contribution to making small-scale experiments at TU Delft successful. We also thank the Faculty of Civil Engineering and Geosciences (CEG) of TU Delft for allowing us to use the water flume in the Hydraulic Engineering Laboratory for these tests. Finally, we thank Visserij Coöperatie Urk (VCU) and Coöperatie Westvoorn (CW) Stellendam for providing details about tickler chain configurations and other practical information.

Authors' contribution

Bithin Ghorai: Conceptualization, Methodology, Formal analysis, Investigation, Writing – Original Draft, Visualization. Justin Tiano: Conceptualization, Methodology, Formal analysis, Investigation, Resources, Writing – Original Draft, Visualization, Project administration. Pieke Molenaar: Methodology, Resources, Writing – Review and Editing. Karline Soetaert: Writing – Review and Editing, Supervision, Funding acquisition. Geert Keetels: Conceptualization, Methodology, Resources, Writing and Review and Editing, Supervision, Project administration, Funding acquisition.

Disclosure statement

The authors declare that they have no known competing financial interests or personal relationships that could have appeared to influence the work reported in this article.

Funding

This work was supported by the Nederlandse Organisatie voor Wetenschappelijk Onderzoek (NWO) [project numbers 18529 and 18523].

ORCID

Bithin Ghorai  <http://orcid.org/0000-0003-0971-8513>

Data availability statement

Some or all data generated or used during the study will be available from the corresponding author by request.

References

- Albiker, J., M. Achmus, D. Frick, and F. Flindt. 2017. 1 g Model Tests on the Displacement Accumulation of Large-Diameter Piles under Cyclic Lateral Loading. *Geotechnical Testing Journal* 40 (2): 173–184. <https://doi.org/10.1520/GTJ20160102>.
- Anonymous. 1990. Effects of Beam Trawl Fishery on the Bottom Fauna in the North Sea. *BEON-Report 8*. Texel, Netherlands: Netherlands Institute for Sea Research, 57.
- Bates, D., M. Mächler, B. Bolker, and S. Walker. 2015. Fitting Linear Mixed-Effects Models Using lme4. *Journal of Statistical Software* 67 (1): 1–48. <https://doi.org/10.18637/jss.v067.i01>.
- Bergman, M. J. N., and M. Hup. 1992. Direct Effects of Beam Trawling on Macrofauna in a Sandy Sediment in the Southern North Sea. *ICES Journal of Marine Science* 49 (1): 5–11. <https://doi.org/10.1093/icesjms/49.1.5>.
- Bi, C. W., Y. P. Zhao, G. H. Dong, T. J. Xu, and F. K. Gui. 2014. Numerical Simulation of the Interaction between Flow and Flexible Nets. *Journal of Fluids and Structures* 45: 180–201. <https://doi.org/10.1016/j.jfluidstructs.2013.11.015>.
- Bolker, B. M., M. E. Brooks, C. J. Clark, S. W. Geange, J. R. Poulsen, M. H. H. Stevens, and J.-S. S. White. 2009. Generalized Linear Mixed Models: A Practical Guide for Ecology and Evolution. *Trends in Ecology & Evolution* 24 (3): 127–135. <https://doi.org/10.1016/j.tree.2008.10.008>.
- Bolton, M. D. 1986. The Strength and Dilatancy of Sands. *Géotechnique* 36 (1): 65–78. <https://doi.org/10.1680/geot.1986.36.1.65>.
- Bridger, J. P. 1972. *Some Observations on the Penetrations into the Sea Bed of Tickler Chains on a Beam Trawl*. ICES, Doc. C.M. 1972/B:7. Gear and Behaviour Committee.
- Cathie, D. N., and J. F. Wintgens. 2001. Pipeline Trenching Using Plows: Performance and Geotechnical Hazards. In *Proceedings of the*

- Offshore Technology Conference, OTC, TX, USA, OTC-13145-MS. <https://doi.org/10.4043/13145-MS>.
- Chakraborty, T., and R. Salgado. 2010. Dilatancy and Shear Strength of Sand at Low Confining Pressures. *Journal of Geotechnical and Geoenvironmental Engineering* 136 (3): 527–532. [https://doi.org/10.1061/\(ASCE\)GT.1943-5606.0000237](https://doi.org/10.1061/(ASCE)GT.1943-5606.0000237).
- Das, B. M. 2010. *Principles of Geotechnical Engineering*. 7th ed. Stamford, CT: Cengage Learning.
- De Borger, E., J. Tiano, U. Braeckman, A. D. Rijnsdorp, and K. Soetaert. 2021. Impact of Bottom Trawling on Sediment Biogeochemistry: A Modelling Approach. *Biogeosciences* 18 (8): 2539–2557. <https://doi.org/10.5194/bg-18-2539-2021>.
- De Groot, S. J. 1995. *On the Penetration of the Beam Trawl into the Sea Bed*. ICES, Doc. C.M. 1995/B:36. Fish Capture Committee.
- Depestele, J., K. Degrendele, M. Esmaeili, A. Ivanović, S. Kröger, F. G. O'Neill, R. Parker, et al. 2019. Comparison of Mechanical Disturbance in Soft Sediments Due to Tickler-Chain Sum Wing Trawl versus Electro-Fitted Pulse Wing Trawl. *ICES Journal of Marine Science* 76 (1): 312–329. <https://doi.org/10.1093/icesjms/fsy124>.
- Depestele, J., A. Ivanović, K. Degrendele, M. Esmaeili, H. Polet, M. Roche, K. Summerbell, L. R. Teal, B. Vanelslander, and F. G. O'Neill. 2016. Measuring and Assessing the Physical Impact of Beam Trawling. *ICES Journal of Marine Science* 73 (Suppl 1): i15–i26. <https://doi.org/10.1093/icesjms/fsv056>.
- Eigaard, O. R., F. Bastardie, M. Breen, G. E. Dinesen, N. T. Hintzen, P. Laffargue, L. O. Mortensen, et al. 2016. Estimating Seabed Pressure from Demersal Trawls, Seines, and Dredges Based on Gear Design and Dimensions. *ICES Journal of Marine Science* 73 (Suppl 1): i27–i43. <https://doi.org/10.1093/icesjms/fsv099>.
- Enerhaug, B. 2011. Contact Forces between Seabed and Fishing Gear Components. In *Proceedings of the 10th International Workshop on Methods for the Development and Evaluation of Maritime Technologies (DEMAT' 11), Split, Croatia. Contributions on the Theory of Fishing Gears and Related Marine Systems*, Vol. 7, 237–246.
- Enerhaug, B., A. Ivanović, F. O'Neill, and K. Summerbell. 2012. Friction Forces between Seabed and Fishing Gear Components. In *Proceedings of the ASME 2012 31st International Conference on Ocean, Offshore and Arctic Engineering, OMAE2012-83395*. Rio De Janeiro, Brazil: ASME, 61–68. <https://doi.org/10.1115/OMAE2012-83395>.
- Esmaeili, M., and A. Ivanović. 2014. Numerical Modelling of Bottom Trawling Ground Gear Element on the Seabed. *Ocean Engineering* 91 (15): 316–328. <https://doi.org/10.1016/j.oceaneng.2014.08.014>.
- Esmaeili, M., and A. Ivanović. 2015. Analytical and Numerical Modelling of Non-Driven Disc on Friction Material. *Computers and Geotechnics* 68: 208–219. <https://doi.org/10.1016/j.compgeo.2015.04.007>.
- Hiddink, J. G., S. Jennings, M. Sciberras, C. L. Szostek, K. M. Hughes, N. Ellis, A. D. Rijnsdorp, et al. 2017. Global Analysis of Depletion and Recovery of Seabed Biota after Bottom Trawling Disturbance. *Proceedings of the National Academy of Sciences* 114 (31): 8301–8306. <https://doi.org/10.1073/pnas.1618858114>.
- Ivanović, A., R. D. Neilson, and F. G. O'Neill. 2011. Modelling the Physical Impact of Trawl Components on the Seabed and Comparison with Sea Trials. *Ocean Engineering* 38 (7): 925–933. <https://doi.org/10.1016/j.oceaneng.2010.09.011>.
- Ivanović, A., and F. G. O'Neill. 2015. Towing Cylindrical Fishing Gear Components on Cohesive Soils. *Computers and Geotechnics* 65: 212–219. <https://doi.org/10.1016/j.compgeo.2014.12.003>.
- Kraan, M., R. Groeneveld, A. Pauwelussen, T. Haasnoot, and S. R. Bush. 2020. Science, Subsidies and the Politics of the Pulse Trawl Ban in the European Union. *Marine Policy* 118 (August): 103975. <https://doi.org/10.1016/j.marpol.2020.103975>.
- Lindeboom, H. J., and S. J. De Groot. 1998. *The Effects of Different Types of Fisheries on the North Sea and Irish Sea Benthic Ecosystems (IMPACT-II) - Report 1998-1/RIVO-DLO Report C003/98*. Texel, The Netherlands: Netherlands Institute for Sea Research, 404.
- Margetts, A. R., and J. P. Bridger. 1971. *The Effect of a Beam Trawl on the Sea Bed*. ICES C.M. 1971/B:8. Gear and Behaviour Committee.
- van Marlen, B., J. A. M. Wiegierinck, E. van Os-Koomen, and E. van Barneveld. 2014. Catch Comparison of Flatfish Pulse Trawls and a Tickler Chain Beam Trawl. *Fisheries Research* 151: 57–69. <https://doi.org/10.1016/j.fishres.2013.11.007>.
- O'Neill, F. G., and A. Ivanović. 2016. The Physical Impact of Towed Demersal Fishing Gears on Soft Sediments. *ICES Journal of Marine Science* 73 (Suppl 1): i5–i14. <https://doi.org/10.1093/icesjms/fsv125>.
- Paschen, M., U. Richter, and W. Köpnick. 2000. *Trawl Penetration in the Sea Bed (TRAPESE)*. Final Report EU Contract 96-006, 150.
- Pitcher, C. R., J. G. Hiddink, S. Jennings, J. Collie, A. M. Parma, R. Amoroso, T. Mazar, et al. 2022. Trawl Impacts on the Relative Status of Biotic Communities of Seabed Sedimentary Habitats in 24 Regions Worldwide. *Proceedings of the National Academy of Sciences* 119 (2): 1–11. <https://doi.org/10.1073/pnas.2109449119>.
- Prakash, K., Sridharan, A., Manoj, N., and Manoj, 2023. Friction Angles of Sands: An Appraisal. *Geotechnical and Geological Engineering*, 841: 4865–4872. <https://doi.org/10.1007/s10706-023-02548-9>.
- Prat, J., J. Antonijuan, A. Folch, A. Sala, A. Lucchetti, F. Sardà, and A. Manuel. 2008. A Simplified Model of the Interaction of the Trawl Warps, the Otterboards and Netting Drag. *Fisheries Research* 94 (1): 109–117. <https://doi.org/10.1016/j.fishres.2008.07.007>.
- Rijnsdorp, A. D., Dol, W., Hoyer, M., and Pastoors, M. A. 2000. Effects of fishing power and competitive interactions among vessels on the effort allocation on the trip level of the Dutch beam trawl fleet. *ICES Journal of Marine Science*, 57(4): 927–937. <https://doi.org/10.1006/jmsc.2000.0580>
- Rijnsdorp, A. D., J. J. Poos, F. J. Quirijns, R. HilleRisLambers, J. W. De Wilde, and W. M. Den Heijer. 2008. The Arms Race between Fishers. *Journal of Sea Research* 60 (1–2): 126–138. <https://doi.org/10.1016/j.seares.2008.03.003>.
- Rijnsdorp, A. D., J. G. Hiddink, P. D. van Denderen, N. T. Hintzen, O. R. Eigaard, S. Valanko, F. Bastardie, et al. 2020. Different Bottom Trawl Fisheries Have a Differential Impact on the Status of the North Sea Seafloor Habitats. *ICES Journal of Marine Science* 77 (5): 1772–1786. <https://doi.org/10.1093/icesjms/fsaa050>.
- Rijnsdorp, A. D., J. Depestele, P. Molenaar, O. R. Eigaard, A. Ivanović, and F. G. O'Neil. 2021. Sediment Mobilization by Bottom Trawls: A Model Approach Applied to the Dutch North Sea Beam Trawl Fishery. *ICES Journal of Marine Science* 78 (5): 1574–1586. <https://doi.org/10.1093/icesjms/fsab029>.
- Tang, M. F., G. H. Dong, T. J. Xu, Y. P. Zhao, and C. W. Bi. 2017. Numerical Simulation of the Drag Force on the Trawl Net. *Turkish Journal of Fisheries and Aquatic Sciences* 17 (6): 1219–1230. https://www.trjfas.org/uploads/pdf_1114.pdf. https://doi.org/10.4194/1303-2712-v17_6_15.
- Tang, M. F., G. H. Dong, T. J. Xu, Y. P. Zhao, C. W. Bi, and W. J. Guo. 2018. Experimental Analysis of the Hydrodynamic Coefficients of Net Panels in Current. *Applied Ocean Research* 79: 253–261. <https://doi.org/10.1016/j.apor.2018.08.009>.
- Valdemarsen, J. W., Jørgensen, T., and Engås, A. 2007. Options to mitigate bottom habitat impact of dragged gears. FAO Fisheries Technical Paper, 506. Rome, FAO, 29.
- Verruijt, A. 2006. *Offshore soil mechanics*. Delft, The Netherlands: Delft University of Technology. <http://OffshoreSMBook.pdf> (verruijt.net).
- Zdravkovich, M. M. 1985. Forces on a Circular Cylinder near a Plane Wall. *Applied Ocean Research* 7 (4): 197–201. [https://doi.org/10.1016/0141-1187\(85\)90026-4](https://doi.org/10.1016/0141-1187(85)90026-4).